Journal of Neurochemistry

JOURNAL OF NEUROCHEMISTRY | 2015 | 134 | 354–370 doi: 10.1111/jnc.13127

ORIGINAL ARTICLE

p35 and Rac1 underlie the neuroprotection and cognitive improvement induced by CDK5 silencing

Rafael Andres Posada-Duque,* Alejandro López-Tobón,* Diego Piedrahita,* Christian González-Billault† and Gloria Patricia Cardona-Gomez*

*Cellular and Molecular Neurobiology Area, Group of Neuroscience of Antioquia, Faculty of Medicine, SIU, Calle 70 N°. 52-21, University of Antioquia UdeA, Medellín, Colombia

†Department of Biology, Faculty of Sciences, Laboratory of Cell and Neuronal Dynamics, Universidad de Chile, Ñuñoa, Santiago, Chile

Abstract

CDK5 plays an important role in neurotransmission and synaptic plasticity in the normal function of the adult brain, and dysregulation can lead to Tau hyperphosphorylation and cognitive impairment. In a previous study, we demonstrated that RNAi knock down of CDK5 reduced the formation of neurofibrillary tangles (NFT) and prevented neuronal loss in triple transgenic Alzheimer's mice. Here, we report that CDK5 RNAi protected against glutamate-mediated excitotoxicity using primary hippocampal neurons transduced with adeno-associated virus 2.5 viral vector eGFP-tagged scrambled or CDK5 shRNA-miR during 12 days. Protection was dependent on a concomitant increase in p35 and was reversed using p35 RNAi, which affected the down-stream Rho GTPase activity. Furthermore, p35 over-expression and constitutively active Rac1 mimicked CDK5 silencing-induced neuroprotection. In addition, 3xTg-Alzheimer's disease mice (24 months old) were injected in the hippocampus with scrambled or CDK5 shRNA-miR, and spatial learning and memory were performed 3 weeks post-injection using 'Morris' water maze test. Our data showed that CDK5 knock down induced an increase in p35 protein levels and Rac activity in triple transgenic Alzheimer's mice, which correlated with the recovery of cognitive function; these findings confirm that increased p35 and active Rac are involved in neuroprotection. In summary, our data suggest that p35 acts as a mediator of Rho GTPase activity and contributes to the neuroprotection induced by CDK5 RNAi.

Keywords: CDK5, neuroprotection, p35, Rho GTPases, RNAi.

J. Neurochem. (2015) **134**, 354–370.

Alzheimer's disease (AD) is the major cause of dementia and is characterized by memory loss, cognitive decline, amyloid β (Aβ) accumulation, the formation of NFT, and progressive neurodegeneration (Querfurth and LaFerla 2010). Cyclin-dependent kinase 5 (CDK5) is a proline-directed serine/threonine kinase; its activation via the p25 protein has been implicated in pathways that lead to neurodegenerative disorders (Kusakawa *et al.* 2000; Cruz *et al.* 2003; Noble *et al.* 2003). CDK5 has received substantial attention (Dhavan and Tsai 2001; Smith *et al.* 2001; Su and Tsai 2011) because this protein is important for cytoskeletal organization, neurite outgrowth, and synaptic plasticity (Patrick *et al.* 1999; Cheung *et al.* 2006). The interaction of CDK5 with p35 or p39, which are both abundantly expressed in neurons, is necessary for activation (Lew *et al.* 1994; Tsai *et al.* 1994). The roles of CDK5 in p35 or p25-dependent processes have been identified; CDK5/p35 is essential for neurodevelopment (Dhavan and Tsai 2001; Cruz *et al.* 2003), whereas CDK5/p25 is involved in neuronal death (Patrick *et al.* 1999). The cleavage of p35 to p25 is

Received July 29, 2014; revised manuscript received April 1, 2015; accepted April 9, 2015.

Address correspondence and reprint requests to Gloria Patricia Cardona-Gómez, Universidad de Antioquia, Sede de Investigación Universitaria (SIU), Calle 62 # 52 – 59; Torre 1, Piso 4, Laboratorio 412; Medellín, Colombia. E-mail: patricia.cardonag@udea.edu.co

Abbreviations used: 3xTg-AD, triple transgenic Alzheimer mice; AAV, adeno-associated virus; AD, Alzheimer's disease; AT8, hyper-phosphorylated tau; CDK5, cyclin-dependent kinase; DIV, day *in vitro*; G-LISA, GTP enzyme-linked immunosorbent assay; GLU, glutamate; GluN, NMDA receptor; IFU, infectious units of virus; LDH, lactate dehydrogenase; MAP-2, microtubule-associated protein-2; PAK, p21-activated kinase; PSD95, postsynaptic density-95; ROCK, Rho kinase; SCR, scrambled; shRNA-miR, short hairpin RNA in a microRNA backbone.

associated with neurodegenerative disorders, such as AD in humans and in mouse models (Patrick *et al.* 1999; Smith *et al.* 2001; Nguyen *et al.* 2002).

CDK5 kinase activity is primarily determined by the amount of p35 in neurons (Takahashi *et al.* 2005). The balance between synthesis and degradation controls the amount of p35 protein. p35 expression is induced by brain-derived neurotrophic factor or nerve-growth factor (Tokuoka *et al.* 2000; Harada *et al.* 2001; Bogush *et al.* 2007); in contrast, p35 degradation by the proteasome is stimulated by excitatory neurotransmission in which glutamate treatment transiently activates CDK5/p35 and results in the phosphorylation of p35 (Wei *et al.* 2005). p35 is phosphorylated by CDK5, resulting in a negative feedback loop for CDK5/p35 regulation (Patrick *et al.* 1998). Furthermore, our previous data demonstrated that silencing CDK5 increases the total levels of p35 in primary neuronal cultures and in wild-type (WT) and AD mouse models (3xTg AD). Although the total levels of p35 are increased, the relative p25/p35 remains similar to control mice (Piedrahita *et al.* 2010). This work suggests that p35 may play a leading role in the effects demonstrated by silencing CDK5.

AD is associated with alterations in the postsynaptic terminals of excitatory glutamatergic synapses (Leuba *et al.* 2014). In the mouse hippocampus, CDK5 phosphorylates the N-terminal domain of postsynaptic density-95 (PSD95) to regulate the synaptic recruitment and clustering of ion channels, particularly K+ channels and *N*-methyl-D-aspartate receptor (GluN)2A and 2B (Fu *et al.* 2001; Morabito *et al.* 2004; Hawasli *et al.* 2007; Plattner *et al.* 2014). PSD-95 is a potential target for protection against ischemic (Tymianski 2011) and AD models (Ittner *et al.* 2010). The proteins identified in the postsynaptic density include cell surface receptors, cytoplasmic signaling enzymes, and cytoskeletal and scaffold proteins. Rho GTPases are among these proteins (Jordan *et al.* 2004; Peng *et al.* 2004).

RhoA and Rac1, which control the actin cytoskeleton, play major roles in neurodevelopment and neuroplasticity. Rho and Rac have been demonstrated to regulate dendrite outgrowth and spine morphogenesis (Hall 1998; Govek *et al.* 2005; Jaffe and Hall 2005; Tada and Sheng 2006). In particular, we proposed that Rho GTPases play a role in neuroprotection (Céspedes-Rubio *et al.* 2010; Posada-Duque *et al.* 2013). Rho GTPases are involved in the response to both tissue damage and survival because these proteins are essential for the morphology and movement of neurons; thus, they play a critical role in the balance between cell survival and death (Semenova *et al.* 2007; Linseman and Loucks 2008; Ma *et al.* 2009). Treatment with a pharmacological inhibitor of RhoA/ROCK blocks the CDK5/p25 activation of the neurodegeneration cascade (Castro-Alvarez *et al.* 2011). In addition, Rac plays critical roles in the protection against excitotoxicity (Gutiérrez-Vargas *et al.* 2010; Posada-Duque *et al.* 2013; Shirao and Gonzalez-Billault 2013).

In previous studies, we proposed CDK5 RNAi-mediated silencing as a novel strategy against the tau pathology associated with AD because the knock down of CDK5 decreased tau phosphorylation, reduced the number of NFT, and blocked the rapid neuronal loss in the hippocampi of older triple transgenic Alzheimer's mice (Piedrahita *et al.* 2010). However, how CDK5 silencing provides this protection remains unclear, and this question is the focus of the present study. Therefore, we evaluated the role of p35 and its relationship with Rho GTPases in the protective action of CDK5 RNAi in a neuronal culture model of glutamate excitotoxicity and a 3xTg AD mouse model.

Materials and methods

Animal procedures

Ten littermate mice (WT) and 28 triple transgenic Alzheimer's (3xTg-AD) mice were used (Oddo *et al.* 2003). The LaFerla Lab donated the parents of the 3xTg-AD and littermate mouse colonies. The animals were housed and raised in a SPF (specific pathogens free) vivarium at SIU–University of Antioquia (Medellin, Colombia) on a 12 : 12 h dark : light cycle; food and water were provided *ad libitum*. The rats and mice were handled according to Law 84 of 1989 and Resolution 8430 of 1993 from the Colombian regulations, as well as Public Law 99-158, November 20, 1985, 'Animals in Research' from the National Institutes of Health.

Primary neuronal cultures

Hippocampal and cortical samples from Wistar rat embryos (E18-19) were dissected, dissociated and cultured on poly-L-lysine (Sigma-Aldrich, St. Louis, MO, USA) pre-coated multi-well plates in Neurobasal medium (Gibco, Rockville, MD, USA), which contained B-27 supplement (Sigma-Aldrich), albumin from a chicken egg (Sigma-Aldrich), N2 human supplement (GIBCO), and a penicillin-streptomycin antibiotic mixture (GIBCO); the samples were cultured at 37°C in a 5% CO_2 humidified atmosphere for a maximum of 19 days *in vitro* (DIV19). Isolated primary neurons were plated at a low density (52 cell/mm^2) for immunofluorescence and at a high density (1500 cell/mm^2) for the Calpain, Rac and RhoA activation assays, western blotting, immunoprecipitation and qPCR.

shRNA-miR AAV viral vector, shRNA lentiviral particles, and transduction

The SCR (scrambled) or CDK5 shRNA-miRs (short hairpin RNA in a microRNA backbone) were designed and validated in our previous study (Piedrahita *et al.* 2010). The adeno-associated virus (AAV) particles were obtained from the Davidson Laboratory (University of Iowa Viral Vector Core). The AAV aliquots were dialysed, and the cells were transduced with 2 μL AAV 2/5 (10 genomes per mL) at a titer of 10^{12} vg/mL for 3 h at 37°C; the media were subsequently completed with B27-supplemented Neurobasal medium. The transductions were performed at DIV7 and maintained for 12 days post-transduction prior to the administration of glutamate and the inhibitor treatments.

p35 shRNA mouse (m) viral particles containing target-specific constructs that encode 19-25-nt (plus hairpin) shRNAs were used to

knock down gene expression (Santa Cruz Biotechnology, Santa Cruz, CA, USA). Commercial control shRNA viral particles encoding a scrambled shRNA sequence that does not specifically degrade any known cellular mRNA were also used. At DIV12, the cultures were transduced for 7 days with lentiviral particles at a titer of 10^6 infectious units of virus in Dulbecco's modified Eagle's medium (DMEM) that contained 25 mM HEPES, pH 7.3.

Transfection and co-transfection of hippocampal cultures

HEK293T cells were co-transfected with pBI-p35/EGFP (enhanced green fluorescent protein) (Utreras *et al.* 2013) and a tTA vector in DMEM with Lipofectamine 2000 (Invitrogen, Carlsbad, CA, USA). At 4 h, the post-transfection medium was replaced with DMEM containing 10% FBS (Fetal bovine serum), and the cells were treated with 2 μg/mL doxycycline (Dox). Hippocampal neurons were transiently transfected with SCR or CDK5 shRNAmiR-pCMV-GIN-ZEO at DIV3, and eGFP-positive neurons from DIV5 were used. The pcDNA3-eGFP-Rac1-WT, pcDNA3-eGFP-Rac1-T17N, pcDNA3-eGFP-Rac1-Q16L, and pBI-p35/eGFP with tTA vector plasmids were transfected and co-transfected into hippocampal neurons with Lipofectamine 2000 (Invitrogen) in Neurobasal medium at DIV5. An equimolar mixture of 0.4 μg of DNA with Lipofectamine 2000 was used. At 4 h, the post-transfection medium was changed for the supplemented Neurobasal medium, and the DIV7 neurons were treated with 125 μM glutamate (20 min) to induce excitotoxicity. After glutamate treatment, the neurons were treated with 10 μM roscovitine (Ros) or 2 μg/mL Dox for 24 h. The DIV8 neurons were fixed for immunofluorescence analyses. The 60 eGFP-positive neurons were used for nucleus and PSD95 cluster quantification (n = 3).

Treatments and inhibitors

DIV7 or DIV18 neurons were treated with 125 μM glutamate (Sigma-Aldrich) for 20 min to induce excitotoxicity (Posada-Duque *et al.* 2013). After 20 min, the glutamate was washed out to evaluate the effects. After 30 min post-glutamate, the proteins were collected for use in the Rho GTPase activation assays; after 12 and 24 h, the proteins were collected or the cells were fixed. For the time course experiment, DIV18 neurons were treated with glutamate, and after 1, 6, 12, 18, and 24 h, the proteins were collected. To evaluate the effects of Ros, DIV7 or DIV18 neurons were treated with a 10 μM Ros (Calbiochem, San Diego, CA, USA) preparation in dimethylsulfoxide (0.01%) mixed in medium. Ros treatment was performed during the 24 h following glutamate excitotoxicity.

Immunofluorescence

Immunofluorescence analysis was performed as previously described (Posada-Duque *et al.* 2013). Briefly, the cells were incubated overnight at 4°C with the following primary antibodies: mouse PSD95 (1 : 250, Calbiochem), rabbit PSD95 (1 : 250, Cell Signaling Technology, Beverly, MA, USA) and mouse MAP2 (1 : 2000, Sigma, St Louis, MO, USA). The Alexa-594 fluorescent antibody was used as a secondary antibody (1 : 1000, Molecular Probes, Eugene, OR, USA). The nuclei were stained with Hoechst 33258 (1 : 5000, Invitrogen), and the cells were incubated with phalloidin conjugated with Alexa 594 (1 : 2000, Molecular probes) for 1 h. The cells were washed 4 times in buffer, coverslipped using Gel Mount (Biomeda, Hatfield, PA, USA), and observed under an Olympus IX 81 (OLYMPUS LATIN AMERICA, INC. Miami, FL, USA) epifluorescence microscope or a DSU (Disk Scan Unit) Spinning Disc Confocal microscope. No staining was observed when the primary antibodies were omitted.

XY images were collected using an Olympus IX 81 microscope with 10X (NA, 0.4), 40X (NA, 1.3) or 60× (NA, 1.42) oil-immersion objectives. Z-stack images were collected at 0.4-μm intervals on an Olympus IX 81 DSU Spinning Disc Confocal microscope (60X oil-immersion; NA, 1.42). The image stacks were deconvolved using Cell^M imaging software (Olympus).

Quantitative image analysis

The percentage of condensed nuclei and the number and length of the neurites were obtained as previously described (Posada-Duque *et al.* 2013). For the PSD95 cluster quantification, we used the eGFP and PSD95 threshold. eGFP sized areas were quantified, and the PSD95 cluster density was obtained after calculating the number of clusters/100 μm^2 eGFP. The average cluster size was obtained from the total area of each cluster divided by the number of fused clusters. All measurements were performed using Image Pro Plus software (Media Cybernetics Inc, Rockville, MD, USA) with 15 neurons per treatment in duplicate assays and at least 4 independent experiments (n = 4).

LDH release

Cytotoxicity was assessed after measuring the lactate dehydrogenase (LDH) released from the cultures using a cytotoxicity detection kit (Roche Molecular Biochemicals, Indianapolis, IN, USA) as previously described (Posada-Duque *et al.* 2013).

Western blotting

After the treatments, the neuron cultures or the medium lateral hippocampus, including the CA1 and dentate gyrus, were homogenized in lysis buffer (Cytoskeleton, Biochem), and Western blotting was performed as previously described (Piedrahita *et al.* 2010). The membranes were incubated overnight at 4°C with the following primary antibodies: rabbit p35 1 : 250 (C-19, Santa Cruz), rabbit CDK5 1 : 250 (Santa Cruz), and mouse AT8 1 : 500 (Pierce, Rockford, IL, USA). βIII tubulin 1 : 5000 (Promega, Madison, WI, USA) was used as a loading control. IRDye 800CW goat anti-mouse or IRDye 680 goat anti-rabbit 1 : 15000 (LI-COR) were used as secondary probes. The blots and images were developed and analyzed using Odyssey Infrared Imaging System application software version 3.0 (LI-COR, Lincoln, NE, USA). The quantification of each blot is presented as the relative units with respect to the loading control values.

In vitro CDK5 kinase assay

Following treatment, the CDK5 activity was measured in 250 μg of total protein from neuronal culture lysates as previously described (Piedrahita *et al.* 2010). CDK5 was immunoprecipitated using 1 μg of an IgG rabbit polyclonal anti-CDK5 antibody (C-8 antibody, Santa Cruz). The antibody and protein extract were rotated overnight at 4°C; protein G Sepharose (Sigma) was subsequently added, and the mixture was incubated for an additional 4 h at 4°C. The washed protein G Sepharose beads were re-suspended in 25 μL kinase assay buffer (20 mM Tris/HCl pH 7.5, 100 μM sodium

orthovanadate, 10 mM $MgCl_2$, 50 mM NaCl, 1 mM dithiothreitol, and 1 mM NaF), and a 10-fold excess (0.5 mM) of ATP was added to the re-suspended beads. Six micromolar calf thymus type III-S histone-1 (H1) from (Sigma) was added as a substrate for CDK5, and the reaction was incubated at 37°C for 30 min. To terminate the reaction, 12.5 μL sodium dodecyl sulfate–polyacrylamide gel electrophoresis loading buffer was added, and the mixture was incubated at 95°C for 5 min. Western blotting detection for CDK5 and phosphorylated rabbit polyclonal anti-H1 (Millipore Corporation, Bedford, MA, USA) were performed. Goat anti-rabbit IRDye 800WE (Li-COR) was applied to the blots and detected using the ODYSSEY Infrared Imaging System (Li-COR). The band intensities for H1 were measured using the Odyssey Infrared Imaging System application software version 3.0 (LI-COR) relative to the CDK5 levels, and CDK5 was measured relative to the IgG heavy chain intensity.

Rac and RhoA activation assays

A Rac and RhoA GTP enzyme-linked immunosorbent assay activation assay kit (Cytoskeleton, Biochem) was used to measure the Rac, RhoA, and Cdc42 activities according to the manufacturer's protocol (Posada-Duque *et al.* 2013).

Calpain activation assay

Cells were homogenized as previously described (Zhu *et al.* 2011). A Calpain-Glo™ protease assay kit (Promega) was used to measure the calpain activity via the manufacturer's recommendations. Human calpain-1 (Tocris-Bioscience, Bristol, BS, UK) was used as a positive control, and the calpain activity from the cell homogenates was measured using a luciferase-based assay on a microplate luminometer (GlioMax, Promega).

CDK5, p35, and GAPDH mRNA analysis

mRNA was purified from neuronal lysates using an RNeasy mini kit (Qiagen, Valencia, CA, USA) and digested with DNase I (Thermoscientific, Waltham, MA, USA). For cDNA synthesis, 0.2 μg of RNA with random primer, Maxime reverse transcriptase and RiboLock inhibitor (Thermo Scientific) were used. The assay conditions for real-time PCR were adjusted for three targets using SYBR–green (Bio-Rad Laboratories, Hercules, CA, USA). Real-time PCR was conducted on a CFX96 Real-time PCR Detection system (BioRad). The CDK5, p35 and GAPDH primer sequences have been described by (Harris *et al.* 1992), (Tsai *et al.* 1994), and (Tsujita *et al.* 2006), respectively. The PCR conditions used to amplify all genes were as follows: 15 min at 95°C and 44 cycles of 95°C for 20 s, 60°C for 30 s, and 72°C for 30 s. After PCR, a melt curve analysis was performed from 60 to 90°C with an increment of 1°C per 0.5 s. The CDK5 and p35 signals were normalized, and the GAPDH (Glyceraldehyde 3-phosphate dehydrogenase) signal (reference gene) was quantified using the relative method.

AAV viral vector administration and the Morris water maze test

WT mice at 18 months of age and 3xTg-AD mice at 24 months of age were injected bilaterally (1 μL) in the hippocampi with an AAV2 viral vector that carried SCR or CDK5 shRNA-miR (the Bregma coordinates were −1.7 antero-posterior, −0.7 lateral and −1.75 depth) for 3 weeks. The injections were performed with a Hamilton syringe (10 μL) at a rate of 0.2 μL/min with a 5-min wait prior to withdrawal of the syringe. The Morris water maze test was performed at 3 weeks post-injection using 3xTg-AD mice, as previously described (Castro-Alvarez *et al.* 2014a). Reversal or transfer test: the mice had to locate a new platform position (opposite the last platform location) to solve a new spatial problem. This test consisted of a second learning session lasting 5 days with 2 trials per day (9 trials in total) and 60 s per trial to locate the hidden platform. A second retention session was performed at 48 h after the last training day (second learning). There was subsequently 1 day with 1 trial per day and 60 s per trial without a platform. During the retention trials, the latency to locate the exact platform location, the number of times the animal crossed the previous platform location, and the distance covered (cm) in the concentric circle with the diameter centered on the platform were recorded. The videos were individually analyzed using View Point software (Lyon, France).

Statistical analyses

The n values used for the *in vitro* and *in vivo* experiments were 3–5 and 5–14, respectively. The parametric data were compared using a multivariable 2-way ANOVA followed by Tukey's *post hoc* test for comparisons between several independent groups. The non-parametric data were analyzed using Kruskal–Wallis and Dunn's Multiple Comparison tests. The comparison between 2 groups was performed using Student's *t*-test for parametric data or the Mann–Whitney test for non-parametric data. All sample groups were processed in parallel to reduce the inter-assay variation. The data are expressed as the means ± SEM. SPSS (Chicago, IL, USA) 17.0 and PRISM (La Jolla, CA, USA) software were used. The results were considered significant with *, $^{\#}$ or $^{+}p < 0.05$, **, $^{\#\#}$ or $^{++}p < 0.01$, ***, $^{\#\#\#}$ or $^{+++}p < 0.001$. *, $^{\#}$ or $^{+}$ directly above the bars represent comparisons between each treatment and the control.

Results

Glutamate excitotoxicity induces p25/p35 protein cleavage and tau hyperphosphorylation in cultured hippocampal neurons

CDK5 activation through the calcium/calpain/p25 pathway plays a key role in neuronal excitotoxicity in AD (Han *et al.* 2005). To determine the rate of change of CDK5 activation after glutamate excitotoxicity, we evaluated a temporal course of p35, p25, and tau hyperphosphorylation using an *in vitro* model. We demonstrated that the treatment of cultured hippocampal neurons with 125 μM glutamate for 20 min induced the cleavage of p35 to produce the p25 fragment 6 h after glutamate treatment, and the maximal levels of p25 were detected at 12 h (Fig. 1a), which is consistent with a peak in tau hyperphosphorylation (AT8). After 12 h of glutamate treatment, the p35, p25, and AT8 levels decayed over time; however, AT8 remained elevated at 24 h (Fig. 1a). These observations were supported by a significant cleavage rate of p25/p35, increased AT8 (Fig. 1b) and active calpain in neurons treated with glutamate at 12 and 24 h (Fig. 1d). Furthermore, at 24 h post-glutamate treatment, the levels of CDK5 and p35 mRNA expression decreased compared with the control (Fig. 1c). Unexpect-

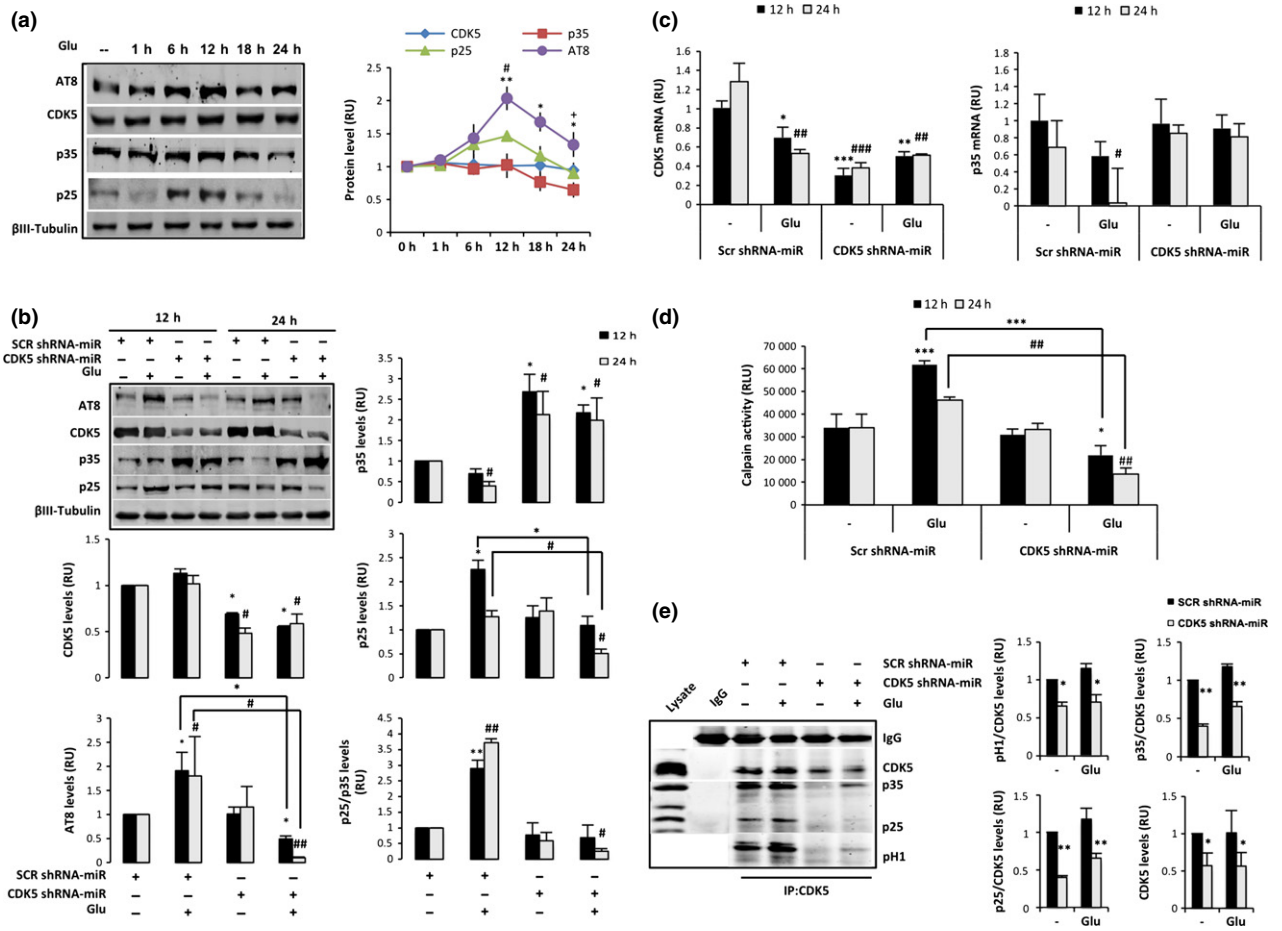

Fig. 1 CDK5 shRNA-miR decreases the p25/p35 cleavage ratio and the tau hyperphosphorylation induced by glutamate excitotoxicity. (a) DIV18 neurons were treated with 125 μM glutamate for 20 min. After 1, 6, 12, 18, and 24 h, the proteins were collected. (b) Primary hippocampal neurons were transduced with SCR or CDK5 shRNA-miR and treated with 125 μM glutamate for 20 min. In (a) and (b), the p35, p25, CDK5 and AT8 protein levels were detected by western blotting. βIII-tubulin was used as the loading control. Relative units = RU, $n = 4$. *, #, + represent comparisons for AT8, p25 and p35, respectively. (c) CDK5 and p35 mRNA expression and (d) calpain activity were measured at 12 and 24 h after glutamate excitotoxicity in neurons transduced with SCR or CDK5 shRNA-miR. Relative light units = RLU, relative units = RU, $n = 5$. (e) CDK5 kinase activity was assessed for 30 min at 24 h. The CDK5 IP and western blot for CDK5, p35, p25, and p-H1 are represented. Negativity for IgG immunoprecipitation was used as an internal control. Representative blots are shown. The intensity quantifications of p35, p25, and p-H1 were relative to CDK5, $n = 3$. All values were normalized to control neurons and are presented as the means ± SEM. *represents comparison between each treatment at 12 h or #24 h. * or $^{+}p < 0.05$, ** or $^{\#\#}p < 0.01$, *** or $^{\#\#\#}p < 0.001$; ANOVA with Tukey's test (b, c, d and e).

edly, the CDK5 activity identified through the H1 phosphorylation rate and the CDK5/p25 and CDK5/p35 association, were not changed after glutamate treatment with respect to the control (Fig. 1e). In addition, the LDH release and the number of condensed nuclei significantly increased after glutamate excitotoxicity at 12 and 24 h (Fig. 2a and b), which confirms p25/p35 cleavage by calpain activation is involved in glutamate excitotoxicity.

CDK5 shRNA-miR protects against glutamate-mediated excitotoxicity

To validate our model based on the CDK5 RNAi, the effect of silencing CDK5 was evaluated in DIV3 hippocampal neurons using SCR or CDK5 shRNA-miR transfection; neurons transfected with CDK5 shRNA-miR for 48 h exhibited significantly fewer secondary and tertiary neurites compared with the SCR shRNA-miR (Figure S1a and b). These observations were supported by previous studies, which demonstrated that CDK5 is required for branching in immature neurons (Cheung *et al.* 2007). However, the effect was different when CDK5 was silenced for 12 days beginning at DIV7 in hippocampal primary cultures and exposure to glutamate-mediated excitotoxicity. Mature neurons transduced with CDK5 shRNA-miR exhibited a silencing of approximately 50% compared with the SCR control, which was supported by a specific reduction in the levels of CDK5 protein and mRNA, in absence or presence of glutamate (Fig. 1b and c). This effect was accompanied by an increase in the p35

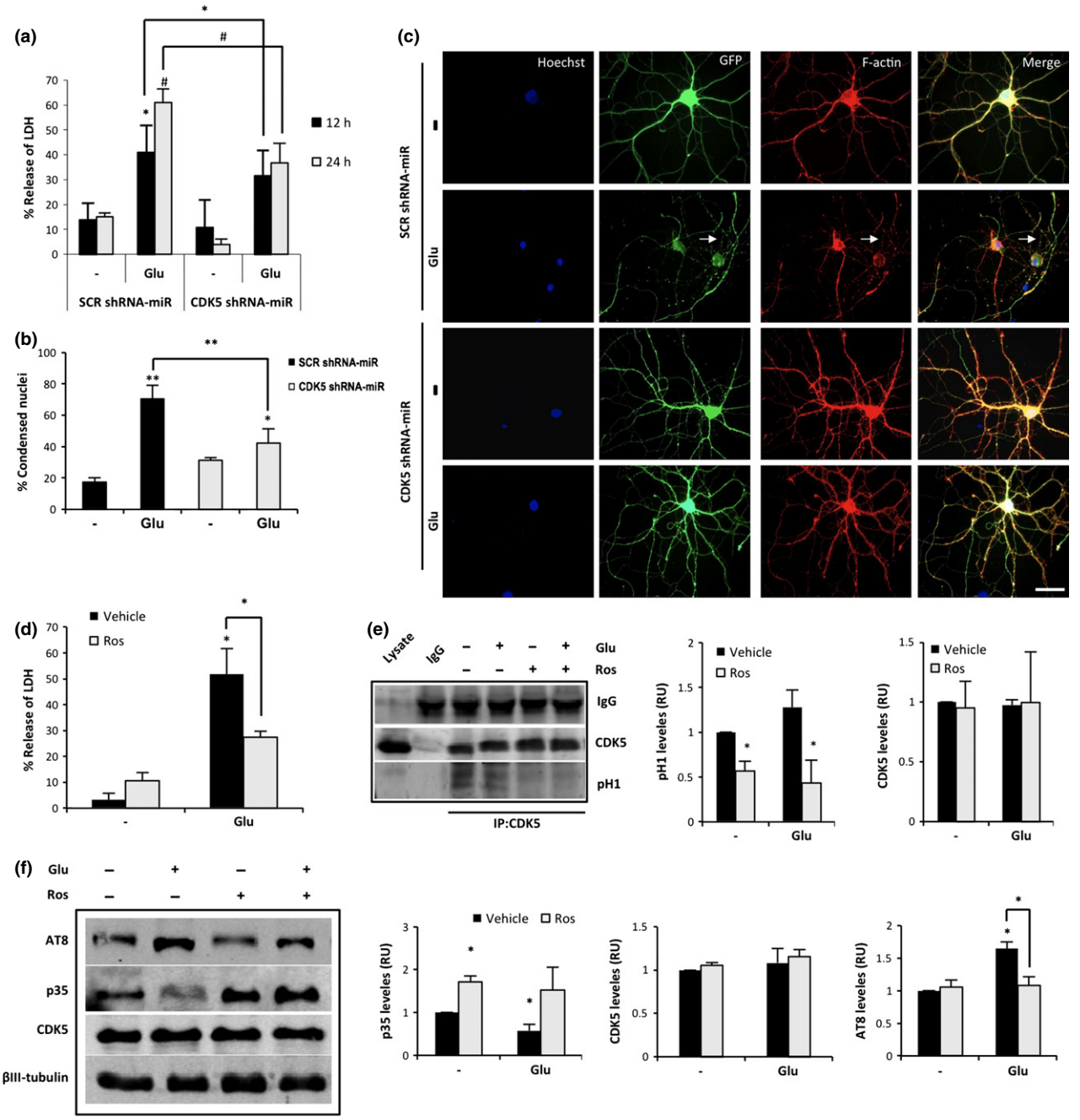

Fig. 2 CDK5 silencing or inhibition protects against glutamate-mediated excitotoxicity. (a) Neuronal cytotoxicity was presented as the percentage of lactate dehydrogenase (LDH) release at 12 and 24 h after glutamate. (b) Percentage of condensed nuclei to total nuclei Hoeschst-positive cells. ($n = 4$). * represents comparison between each treatment at 12 h or # at 24 h * or # $p < 0.05$, ** $p < 0.01$; ANOVA with Tukey's test for a and b. (c) Morphological characteristics indicate adeno-associated virus (AAV) vector viral eGFP-tagged SCR and CDK5 shRNA-miR (green). The arrows represent a discontinuous pattern that resembles the actin depolymerization processes in the glutamate-treated cells. Scale bar, 20 μm, $n = 5$. (d) Neuronal cytotoxicity, (e) CDK5 activity and (f) p35 and CDK5 protein levels were determined from hippocampal neurons (DIV18) treated with 125 μM glutamate for 20 min, followed by 10 μM Ros for 24 h. The data are presented as the means ± SEM of $n = 4$ per triplicate. All values were normalized to the control neurons. *$p < 0.05$; ANOVA with Tukey's test.

protein levels and a p35 mRNA recovery after glutamate treatment (Fig. 1b and c); however, the p25/p35 ratio remained constant, which indicates that there were no changes in the p35-p25 cleavage in cells transduced with CDK5 shRNA-miR alone (Fig. 1b). Interestingly, CDK5 shRNA-miR drastically decreased the ratio of p25/p35 cleavage, the hyperphosphory-

Fig. 3 CDK5 shRNA-miR-induced neuroprotection required p35. (a) CDK5 kinase activity was assessed for 30 min. CDK5 IP and western blot analyses of CDK5 and p-H1 are represented. Quantification of the intensity of CDK5 and p-H1 proteins was performed. RU, relative units. $n = 3$. (b) Neuronal cytotoxicity is presented as the percentage of lactate dehydrogenase (LDH) release. The data are presented as the means ± SEM of $n = 3$. (c) Calpain activity at 24 h after glutamate excitotoxicity in neurons transduced with SCR or CDK5 shRNA-miR or with control or p35 shRNA. Relative light units = RLU. (d) The p35, p25, p35/p25 ratio, CDK5 and AT8 protein levels. (e) CDK5 and p35 mRNA expression at 24 h after glutamate excitotoxicity in neurons transduced with SCR or CDK5 shRNA-miR or with control or p35 shRNA. Relative units = RU, $n = 5$. All values were normalized to the control neurons and are presented as the means ± SEM. Control shRNA: black bars and p35 shRNA: gray bars. *represents comparison between each treatment of control shRNA neurons or $^{\#}$p35 shRNA neurons. * or $^{+}p < 0.05$, ** or $^{\#\#}p < 0.01$, *** or $^{\#\#\#}p < 0.001$; ANOVA with Tukey's test (a, b and d) or Kruskal–Wallis test with Dunn's analysis (c and e).

lation of tau and the level of active calpain induced by glutamate excitotoxicity at 12 and 24 h (Fig. 1b and d). Consistently, transduction with the CDK5 shRNA-miR decreased the p35 and p25 associated with CDK5 under both basal and excitotoxic conditions, which is consistent with a decrease in CDK5 activity through a reduction in p-H1 at 24 h after glutamate treatment (Fig. 1e). Neurons treated with glutamate exhibited increased LDH, greater percentages of condensed nuclei, and altered actin cytoskeletons in terms of their beaded and fragmented processes relative to the controls (Fig. 2 b and c). The CDK5 shRNA-miR prevented the release of LDH and alterations in the neuronal morphology at 24 h (Fig. 2a and c). These effects were confirmed by pharmacological inhibition of CDK5 using Ros, which reversed the increase in LDH release in response to glutamate, supported by the decrease in CDK5 activity, similar to the effects obtained with CDK5 silencing (Fig. 2D and E). Furthermore, neurons treated with Ros exhibited an increased p35 level, even after glutamate excitotoxicity, when AT8 was also reduced (Fig. 2f). These findings demonstrate that CDK5 silencing induces neuroprotection and reduces glutamate-induced tau hyperphosphorylation via the reduction in cleavage of p35 to p25; these findings support p35 as a specific target of the reduced availability of CDK5.

CDK5 shRNA-miR-induced neuroprotection requires p35

It was recently suggested that p10 is a pro-survival domain in p35, which is essential for normal CDK5/p35 function in neurons (Zhang *et al.* 2012; Shukla *et al.* 2013). Therefore, the role of p35 in CDK5 shRNA-miR-induced neuroprotection was analyzed through co-transduction of CDK5 shRNA-miR AAV2 and p35 shRNA lentiviral particles delivered at DIV7 for 12 days and at DIV12 for 7 days, respectively (Fig. 1c). CDK5 was immunoprecipitated, and reduced CDK5 activity was identified by the H1 phosphorylation rate in neurons transduced with CDK5 shRNA-miR compared with the SCR control (Fig. 3a). Although we detected a 50% reduction in CDK5 activity after silencing CDK5 in basal and glutamate-treated neurons compared with the control (Fig. 3a), the reduction was sufficient to achieve protection in a glutamate-induced excitotoxicity model (Fig. 3b). However, the neurons transduced with p35 shRNA, which exhibited decreased p35, also achieved a 50–60% reduction in CDK5 kinase activity (Fig. 3a and d), which confirms that CDK5 activity is p35-dependent. In addition, we demonstrated that p35 shRNA blocked the CDK5 RNAi-induced neuroprotection because p35 shRNA reversed the reduction of LDH release and calpain activation in response to glutamate excitotoxicity after transduction with CDK5 shRNA-miR (Fig. 3b and c). As previously indicated, the silencing of CDK5 decreased the cleavage of p35 to p25 (Fig. 3d), which was induced by glutamate in the control lentiviral particle (Fig. 3c and d). Interestingly, p35 silencing decreased the p25 and AT8 levels; however, the decreased p25 and AT8 levels were not sufficient for neuroprotection (Fig. 3b and d). Thus, p35 was necessary for the induction of tau hyperphosphorylation by CDK5 in the context of glutamate excitotoxicity, despite the increased LDH and calpain activities (Fig. 3). To validate the knockdown of p35 by p35 shRNA, p35 mRNA was determined, and the neurons of all treatments co-transduced with p35 shRNA exhibited a specific silencing of p35 mRNA (Fig. 3e). These results suggest that CDK5 shRNA-miR-induced neuroprotection requires p35.

p35 over-expression induces neuroprotection

To validate the inducible over-expression of p35, we co-transfected pBI-p35 and the tTA vector with (Tet-OFF) or without (Tet-ON) dox in HEK293T cell cultures. The cells with pBI-p35 Tet-OFF exhibited a specific increase in p35 levels compared with the p25 levels (Fig. 4a). The neurons were subsequently co-transfected with pBI-p35 and tTA to analyze the role of p35 in the context of Ros-induced neuroprotection. Neurons transfected with a GFP empty vector exhibited typical hallmarks of glutamate excitotoxicity, including an increased number of condensed nuclei and increased accumulation of PSD95 clusters, which corresponded to an aberrant PSD95 equivalent to a larger PSD95 area cluster (Fig. 4b–d); these changes were reversed by Ros (Fig. 4b–d). Similarly, neurons co-transfected with the pBI-p35 Tet-OFF version exhibited indicators of degeneration with glutamate and a significant decrease in the number of condensed nuclei with Ros (Figs 4b and S2). Surprisingly, neurons with pBI-p35 Tet-ON exhibited decreased nuclear condensation during all treatments, even glutamate treatment (Fig. 4b and d). Furthermore, these neurons exhibited a pattern of PSD95 clustering similar to the control (Fig. 4c and d), which supports the idea that p35 *per se* protects and underlies Ros-induced neuroprotection.

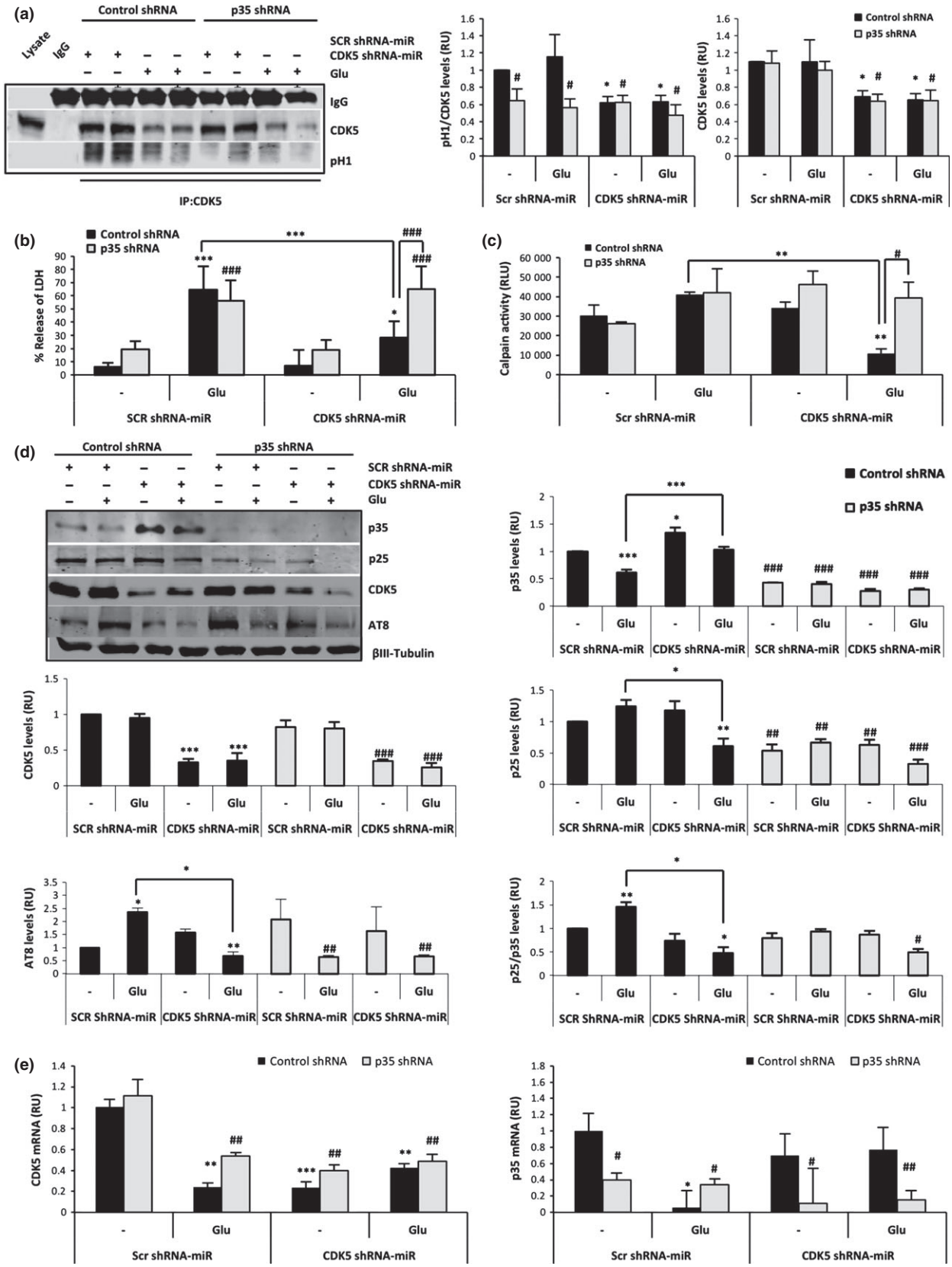
(a)
Control shRNA
p35 shRNA
Lysate
IgG
SCR shRNA-miR
CDK5 shRNA-miR
Glu
IgG
CDK5
pH1
IP:CDK5
pH1/CDK5 levels (RU)
CDK5 levels (RU)
Scr shRNA-miR
CDK5 shRNA-miR
(b)
% Release of LDH
(c)
Calpain activity (RU)
(d)
p35
p25
CDK5
AT8
βIII-Tubulin
p35 levels (RU)
p25 levels (RU)
CDK5 levels (RU)
AT8 levels (RU)
p25/p35 levels (RU)
(e)
CDK5 mRNA (RU)
p35 mRNA (RU)

CDK5 shRNA-miR-induced neuroprotection requires p35 to regulate Rho GTPases

The membrane localization of p35 and its subsequent effect on CDK5 activity have been suggested to be dependent on Rac1 (Sananbenesi *et al.* 2007), and RhoA/ROCK inhibition were associated with a decrease in CDK5/p25 formation (Castro-Alvarez *et al.* 2011). Therefore, to determine the role of Rho GTPases in CDK5 shRNA-miR-induced neuroprotection, CDK5 and p35 were knocked down in cells exposed to glutamate. The neurons treated with glutamate exhibited decreased Rac activity (Fig. 5a) but increased RhoA activity (Fig. 5b), which were reversed after CDK5 silencing (Fig. 5a and b). Moreover, CDK5 shRNA-miR, either alone or via its neuroprotective effect, induced the up-regulation of active Rac (Fig. 5b). Interestingly, the CDK5 shRNA-miR-induced Rac activity involved in neuroprotection was blocked by p35 shRNA, and under these conditions, RhoA activity increased (Fig. 5a and b). We subsequently analyzed the role of Rac1 activation in Ros-induced protection in neurons transfected with WT, dominant negative (T17N), and constitutively active (Q16L) versions of Rac1. All neuronal groups transfected with the T17N-Rac1 exhibited a significant increase in the number of condensed nuclei in contrast to the neurons transfected with Q61L-Rac1, which exhibited decreased nuclear condensation during all treatments, even compared with WT-Rac1 glutamate treatment (Fig. 5c), suggesting that Ros requires active Rac to be neuroprotective. Taken together, these results indicated that CDK5 shRNA-miR-induced neuroprotection requires p35 up-regulation to activate Rac1.

CDK5 shRNA-miR increases p35 and Rac activity in WT and 3xTg-AD mice, which is correlated with improved memory skills

The induction of synaptic plasticity and hippocampal-dependent spatial learning is affected in CDK5 and p35 transgenic and knockout mice (Ohshima *et al.* 2005; Wei *et al.* 2005; Hawasli *et al.* 2007). We sought to determine whether the modulation of p35 and Rac activity through CDK5 RNAi could be related to cognitive performance. Learning and spatial memory were evaluated in 24-month-old 3xTg-AD mice injected in the hippocampal CA1 area with CDK5 shRNA-miR or SCR shRNA-miR as a control for 3 weeks. During the visible platform test, the CDK5 shRNA-miR-treated 3xTg-AD mice did not exhibit differences compared with the controls (Fig. 6a). In the learning test, although the CDK5 shRNA-miR-treated 3xTg-AD mice did not exhibit a significant difference in their ability to locate the hidden platform compared with the SCR control, in the retention test, the CDK5 shRNA-miR-treated 3xTg-AD mice spent less time searching for the hidden platform (Fig. 6a). Spatial acuity is a more sensitive parameter used to measure spatial learning, which is demonstrated by the ability to find the specific hidden platform location; the CDK5 shRNA-miR-treated 3xTg-AD mice increased the number of platform area crossings and increased the time and distance travelled in the test with the hidden platform location compared with the SCR control, which confirms that CDK5 silencing improved the spatial memory of these animals (Fig. 6b). Moreover, in the reversal-learning test, the 3xTg-AD mice with CDK5 shRNA-miR exhibited a significantly shorter latency time to learn the new position, particularly on days 7 and 8 (Fig. 6c). Furthermore, in the retention after the reversal learning, the CDK5 shRNA-miR 3xTg-AD mice spent less time finding the former position of the platform compared with the control group (Fig. 6c). However, the CDK5 shRNA-miR-treated 3xTg-AD mice did not exhibit differences compared with the controls when spatial acuity was evaluated after reversal learning; the CDK5 shRNA-miR mice exhibited interest in looking for the initial and final platforms in the learning and reversal tests, respectively (Fig. 6d). We subsequently determined the modulation of PSD95, the p35 protein levels, and the Rac activity in the brains of these CDK5 shRNA-miR-treated 3xTg-AD mice with improved memory performance, as well as in non-trained wild-type mice. CDK5 was silenced in both the WT and 3xTg-AD mice injected with CDK5 shRNA-miR, which resulted in a significant increase in PSD95, p35, and Rac activation compared with the control values (Fig. 6e and f). Taken together, these results support the findings that CDK5 shRNA-miR improves memory function in 3xTg-AD mice and also correlates with p35 up-regulation and Rac activity.

Discussion

For the first time, our data suggest that p35/Rac1 signaling is critical in the CDK5 shRNAmiR-induced neuroprotection against glutamate neurotoxicity and is also correlated with the recovery of cognitive function in 3xTg-AD mice. Various pharmacological inhibitors of CDK5 have also been demonstrated to exert a protective function. The inhibition of CDK5 with roscovitine, a small molecule CDK5 inhibitor (Lopes *et al.* 2007; Timsit and Menn 2012), protects against kainic acid-induced excitotoxicity in cultured hippocampal neurons (Putkonen *et al.* 2011; Park *et al.* 2012); a novel CDK5 inhibitor of the diaminothiazole class ameliorates Tau pathology in old 3xTg-AD mice (Zhang *et al.* 2013). Furthermore, CDK5 inhibition protects against Tau protein-related pathology (Liu *et al.* 2003; Lopes *et al.* 2007; Piedrahita *et al.* 2010).

The benefits of CDK5 silencing were accompanied by increased levels of p35, reduced CDK5 activity and decreased levels of active calpain, which was p35 dependent. Truncated peptides of various lengths derived from p35 have been successful in the specific reduction of CDK5 hyperactivity *in vitro* in cell cultures (Zheng *et al.* 2005, 2010) and have been

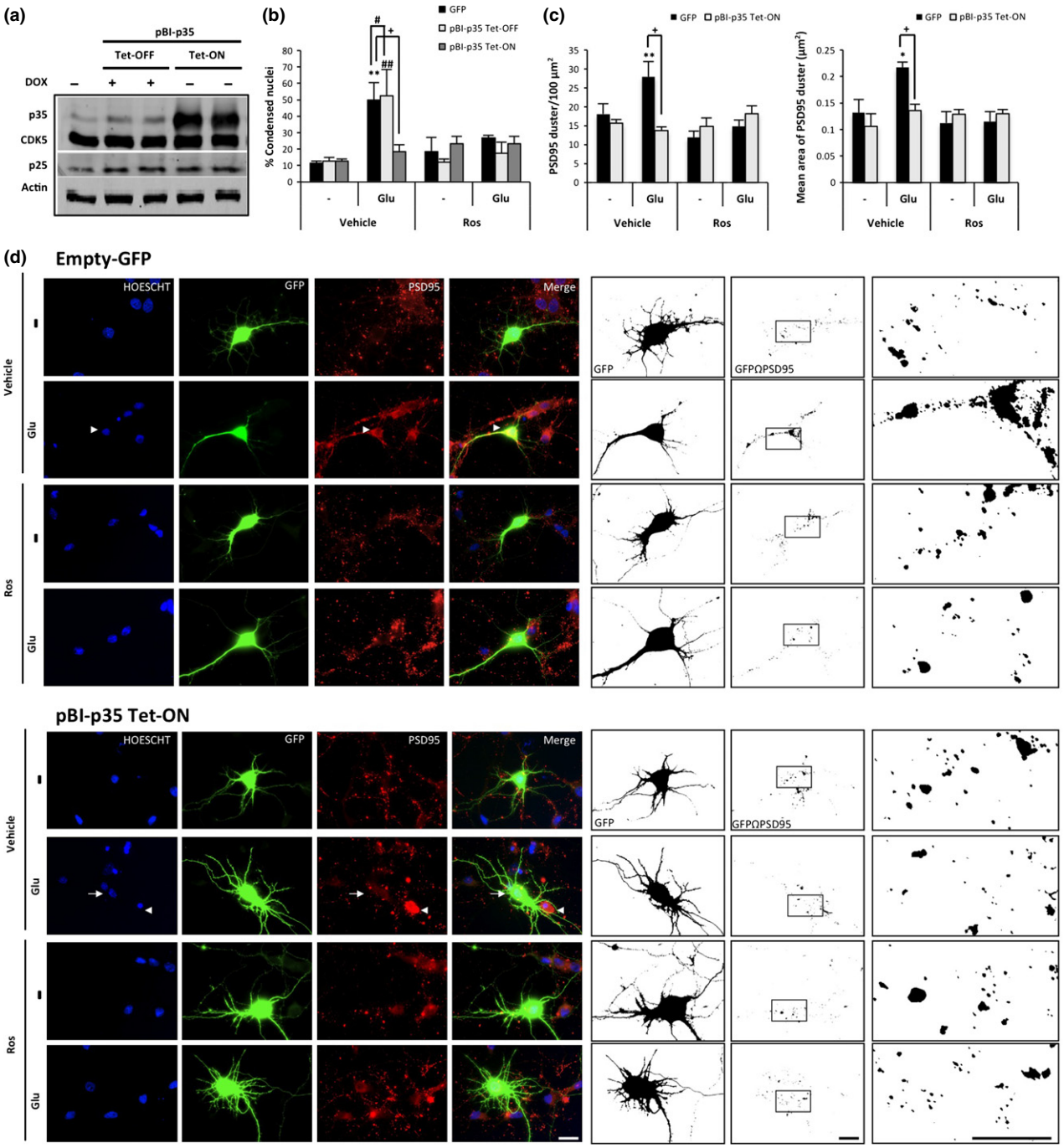

Fig. 4 p35 over-expressed and CDK5 inhibition protects against glutamate excitotoxicity. (a) Hippocampal neurons (DIV5) were co-transfected with pBI-p35/eGFP –tTA, and (b) the percentage of condensed nuclei relative to the total nuclei from the transfected neurons were treated (DIV7) with 125 μM glutamate for 20 min, followed by 10 μM Ros for 24 h. p35 and CDK5 protein levels were detected by western blotting; β-actin was used as the loading control. eGFP: black bars, Tet-OFF: gray bars and Tet-ON: bright gray bars. (c) The number and area of postsynaptic density-95 (PSD95) clusters in transfected neurons. The data are presented as the means ± SEM of $n = 3$, by duplicate. *, $^{\#}$, or $^{+}$ represent the comparisons between each treatment of: eGFP, Tet-OFF and Tet-ON, respectively. *, $^{\#}$ or $^{+}$ $p < 0.05$, **, $^{\#\#}$ or $^{++}p < 0.01$, ***, $^{\#\#\#}$ or $^{+++}p < 0.001$; ANOVA with Tukey's test. (d) The morphological characteristics are shown for the neurons transfected with GFP-tagged plasmids (green), empty-GFP and pBI-p35 Tet-ON. Nuclei were stained with Hoechst (blue), and PSD95 was labeled with Alexa 594 dye (red). The arrowhead shows the condensed nucleus compared with the normal nucleus (arrow). Magnification, 60X. Scale bar, 20 μm. Binary images were used to determine the number and area of the PSD95 clusters on GF- positive neurons. Magnification, 60X with 50% zoom. Scale bar, 20 μm. $n = 3$ per duplicate.

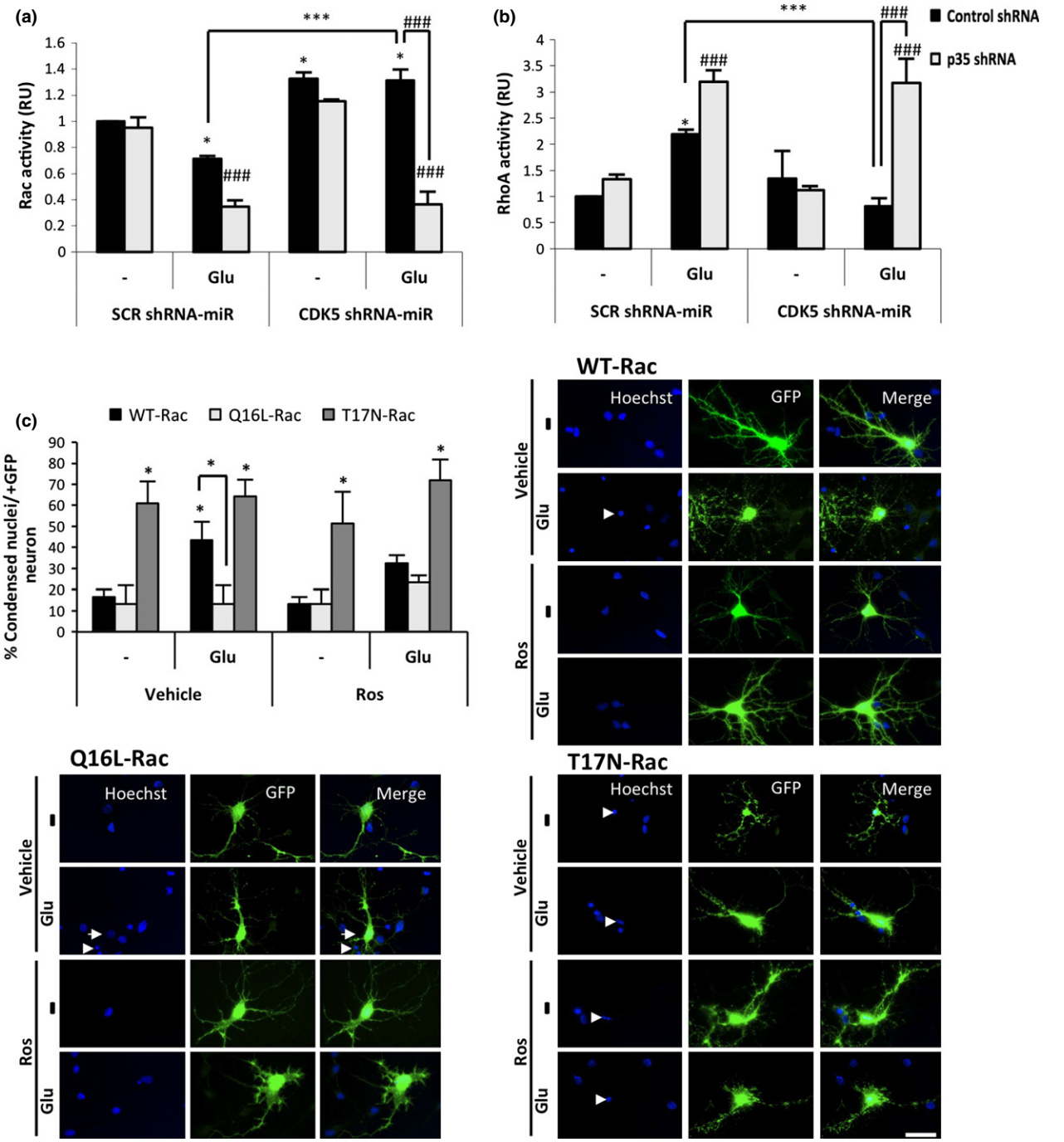

Fig. 5 CDK5 shRNA-miR-induced neuroprotection is mediated by p35 and active Rac1. (a) Rac and (b) RhoA activity were quantified after a 30 min of glutamate treatment as the amount of Rac-GTP and RhoA-GTP by ELISA (λ = 490 nm). The data are presented as the means ± SEM from $n = 3$ per duplicate. Control shRNA: black bars and p35 shRNA: gray bars. *represents the comparison between each treatment of the control shRNA neurons or # p35 shRNA neurons. * or $^{+}p < 0.05$, *** or $^{\#\#\#}p < 0.001$; ANOVA with Tukey's test (a and b). (c) Percentage of condensed nuclei relative to the total nuclei from transfected neurons. WT: black bars, QA: bright gray bars and DN: gray bars. Data are presented as the mean ± SEM ($n = 3$), and each experiment was performed in duplicate. The morphological characteristics are shown for the cortical neurons transfected with GFP-tagged plasmids (green) that expressed three versions of Rac1: wild-type (WT), dominant negative (T17N) and constitutively active (Q61L). The nuclei were stained with Hoechst (blue). The arrowhead shows the condensed nucleus compared with the normal nucleus (arrow). Magnification, 60X. Scale bar, 20 μm ($n = 5$). The arrowhead shows the condensed nucleus compared with the normal nucleus (arrow). Asterisks directly above the bars represent comparisons between each treatment and the buffer control. *$p < 0.05$; Kruskal–Wallis test with Dunn's analysis.

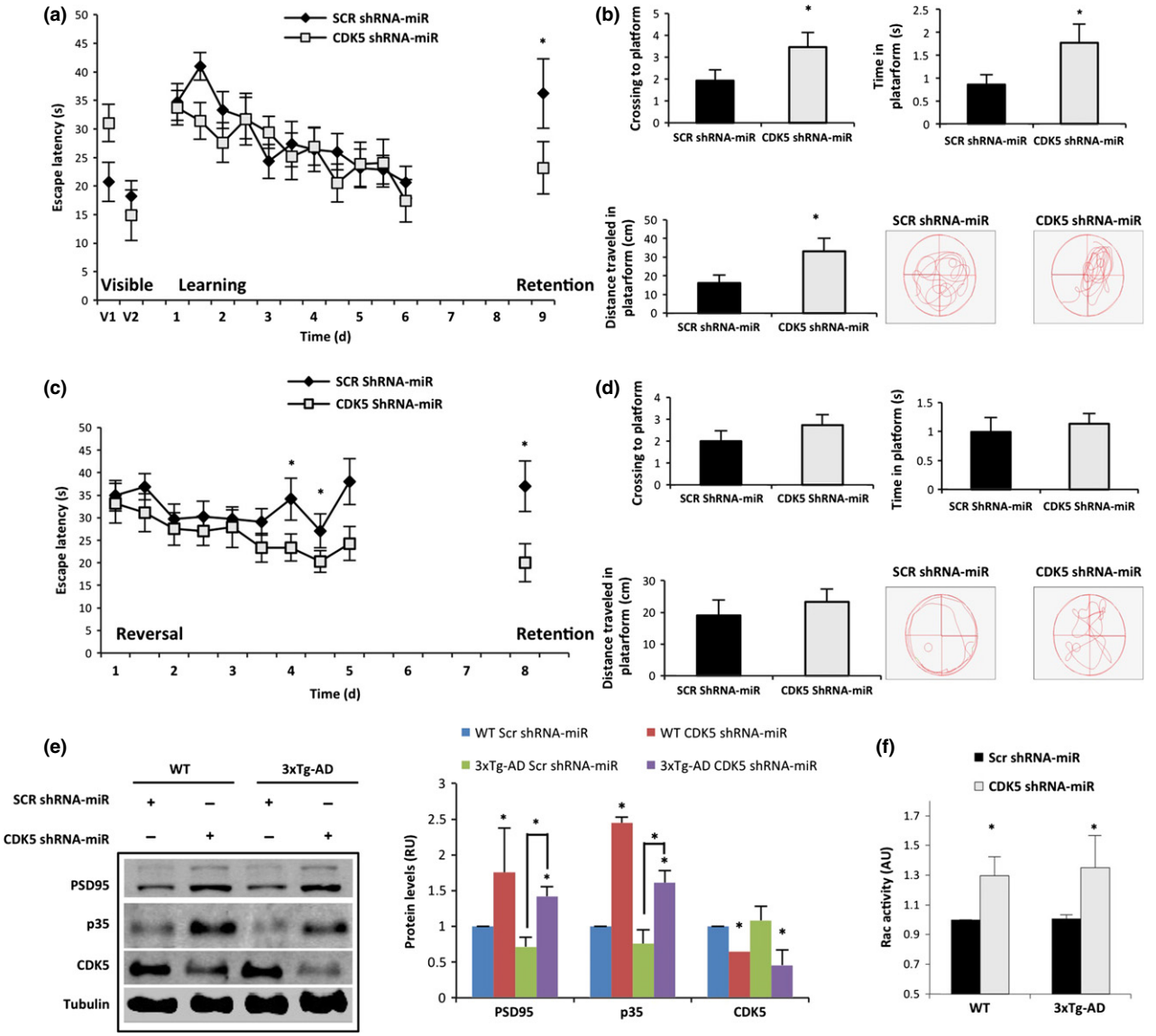

Fig. 6 CDK5 miR improves learning and memory in 3xtg-Alzheimer's disease (AD) mice that exhibit increased p35 and active Rac. The test procedure comprised the (a) visible test, learning and retention with a hidden platform. (b) Spatial acuity was represented as the number of platform area crossings and the time and distance travelled to the hidden platform location in the retention test. (c and d) Reversal learning test with a second retention. Analysis of the latency in (c) and spatial acuity measurements in (d). Data are presented as the mean ± SEM $n = 14$. $^*p < 0.05$. (e) postsynaptic density-95 (PSD95), p35, and CDK5 protein levels from the hippocampus assessed via western blotting. βIII-tubulin was used as the loading control. Relative units = RU. F) Rac activity was quantified by ELISA (λ = 490 nm). The data are presented as the means ± SEM from $n = 5$ per duplicate. The values were normalized to the control. $^*p < 0.05$; Student's *t*-test (a, b, c, d and f). $^*p < 0.05$; ANOVA with Tukey's test for (e).

shown to prevent AD phenotypes in mouse models (Shukla *et al.* 2013). Specifically, p10, the N-terminal domain of p35, is a unique pro-survival domain that is essential for normal CDK5/p35 function in neurons. The loss of the p10 domain results in CDK5/p25 toxicity and neurodegeneration (Zhang *et al.* 2012). In addition, during neuronal differentiation with retinoic acid, ERK (extracellular-signal-regulated kinase)/erg-1 activation increases p35 transcription; CDK5 subsequently acts up-stream of ERK to inhibit the production of p35 (Lee and Kim 2004). During development, the p35 levels are finely regulated through the ubiquitin-proteasome system, and the CDK5 phosphorylation of p35 reduces the protein stability and signal for degradation (Patrick *et al.* 1999; Saito *et al.* 2007). Therefore, the findings suggest that CDK5 silencing in a p35-dependent mode prevented the cleavage of p35 to p25, reduced the CDK5 activity, and decreased the calpain activation, which are key components of neurotoxicity and cell death. Many evidences indicate that CDK5 is a target of calpain; however,

how CDK5 can impact calpain, remain unclear. The calpain activation is mediated by Ca^{2+}, in fact, the imbalance of intracellular Ca^{2+} occurs both, *N*-methyl-D-aspartate and α-amino-3-hydroxy-5-methylisoxazole-4-propionate-mediated Ca^{2+} entrance, and by Ca^{2+} release from mitochondria and ER, process which are favored by CDK5 (Li *et al.* 2001; Wang *et al.* 2003; Kerokoski *et al.* 2004; Darios *et al.* 2005). In this sense, CDK5 silencing could avoid p35 degradation and thereby exert a pro-survival effect (Fig. 7). Furthermore, p35 is also required for the production of p25 and the ability of CDK5 to phosphorylate tau; however, the reduction of hyperphosphorylated tau was not sufficient to prevent cell death. These data are emphasized by the crucial role of p35 in survival.

We also demonstrated that CDK5 silencing decreased the CDK5/p35 and CDK5/p25 associations, which suggests that p35 may have a role in survival in addition to regulating CDK5 activity. The exogenous addition of p35 increases CDK5 activity both *in vitro* and *in vivo* (p35 transgenic mice) (Tanaka *et al.* 2001); furthermore, it has been demonstrated that p35 associates with different cytoskeletal proteins without CDK5 (Hou *et al.* 2007). In addition, the N-terminal domains of p35 are specific for association with Rac1 and p21-activated kinase (PAK)1 (Nikolic *et al.* 1998), and the presence of p35 is required for the membrane function of PAK1 to regulate neuronal morphology. One potential mechanism of action of the p35 or p10 domain in survival has been proposed as the requirement of an inhibitory complex that comprises endogenous p10, p25, CDK5, and possibly Prx2 (Zhang *et al.* 2012). Thus, we propose a novel role of p35 in the regulation of Rho GTPases, which is required for neuroprotection.

The mechanism of CDK5 silencing protection involves Rho GTPases. CDK5 silencing induces the differential regulation of Rho GTPase, which promotes Rac activity and suppresses RhoA activity. Rho GTPases have been implicated in survival and neuroprotection, active Rac1 is crucial for survival (Gutiérrez-Vargas *et al.* 2010; Posada-Duque *et al.* 2013), and RhoA is involved in neuronal death progression (Semenova *et al.* 2007). Active Rac1 leads to the activation of PAK and PI3K. PAK signaling stimulates neurite outgrowth, synapse formation, and activity-dependent Ca^{2+} signaling, which promote neuronal survival; PI3K induces the activation of Akt A (also known as Protein kinase B (PKB)), which promotes survival via the phosphorylation and inhibition of several pro-apoptotic proteins and influences neurite outgrowth (Linseman and Loucks 2008; Read and Gorman 2009). CDK5/p35 activity prevents extinction associated with emotional trauma, in part through the inhibition of PAK1 activity in a Rac1-dependent manner (Sananbenesi *et al.* 2007). Furthermore, CDK5/p35 phosphorylation of ras guanine nucleotide releasing factor 2

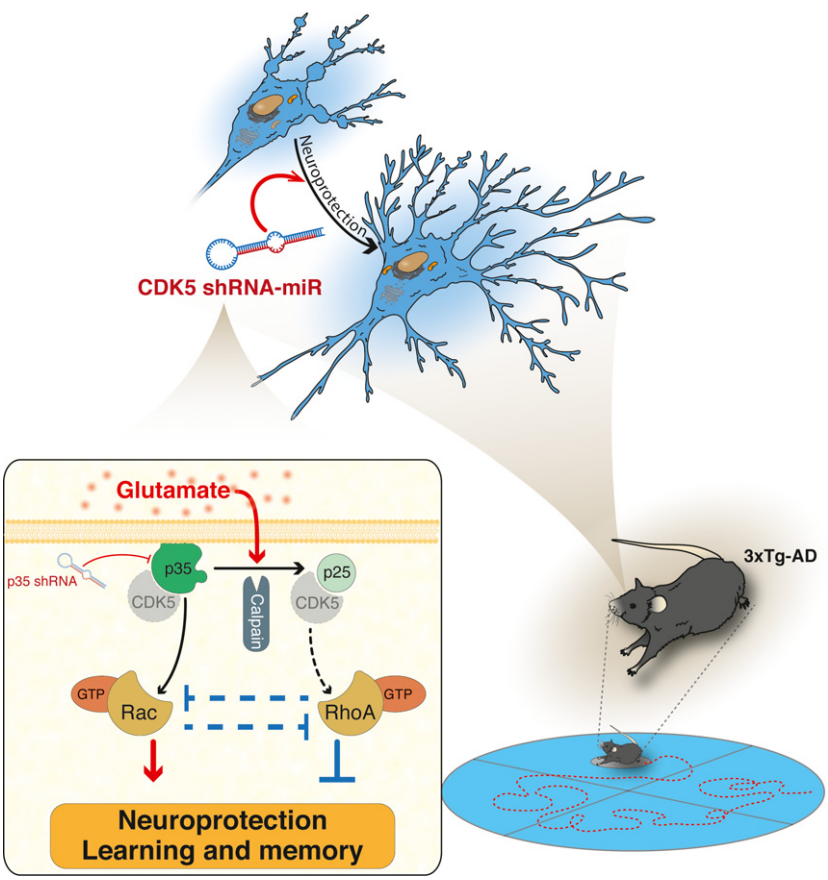

Fig. 7 Hypothetical schematic model: CDK5 RNAi-induced protection and cognitive improvement in a pathological context that depended on the p35/Rac1 GTPase pathway. CDK5 shRNAmiR blocks calpain activation and the cleavage of p35 to p25 produced by glutamate, which generates neuroprotection in a p35 up-regulation dependent mode and its downstream control of Rho GTPases, such as Rac1 and RhoA.

(RasGRF2) mediates a reduction in Rac activity (Kesavapany *et al.* 2004). Therefore, Rac1 activation through p35 up-regulation is necessary for neuronal survival and neuroprotection induced by CDK5 silencing or inhibition (Fig. 7).

Rho/ROCK signaling plays a central role in neuronal injury and disease. During ischemia or excitotoxicity, a p38alpha MAPK-dependent pro-apoptotic signaling cascade is induced, which enhances neuronal injury (Trapp *et al.* 2001; Semenova *et al.* 2007). In addition, in AD, Rho/ROCK activity promotes Aβ production through amyloid precursor protein processing, and ROCK inhibition reduces Aβ levels in AD transgenic mice (Mann *et al.* 1996; Zhou *et al.* 2003). Our previous report demonstrates that CDK5/p25 is associated with cognitive impairment and tauopathy, which were prevented by ROCK inhibition (Castro-Alvarez *et al.* 2011). The abnormal activity of CDK5/p25 and increased RhoA/ROCK activity associated with neurodegeneration suggest that the therapeutic effect of CDK5 silencing involves pro-survival signaling through Rac and the reversion of the RhoA/ROCK-activated pro-apoptotic pathway (Fig. 7).

The suppression of p35 exerts deleterious effects on neurons after excitotoxic injury. The p35 downstream signaling involves neuronal survival pathways through PI3K/Akt or the negative regulation of apoptotic pathways, such as JNK3/MAPK p38a (Li *et al.* 2001, 2003). Furthermore, p35 is required for ERK½ activation, which induces up-regulation of Bcl2, a known anti-apoptotic factor (Wang *et al.* 2005; Zheng *et al.* 2007). The p35 deletion is associated with vacuolar pathology, progressive cell death and increased formation of autophago-lysosomes in Drosophila brains, which supports a neurodegenerative phenotype (Trunova and Giniger 2012). The close relationship between survival and active Rac as cell death and active RhoA, which were up-regulated or inhibited by CDK5 silencing, respectively, were reversed by the reduction of p35 using p35 shRNA; thus, these findings support the critical role of p35 for survival via the modulation of Rho GTPase.

In addition, our findings suggest that the glutamate excitotoxicity-induced increase in PSD95 clusters corresponds to aberrant postsynaptic features, which supports a previous study that demonstrated an increase in PSD95 in the entorhinal and frontal cortices of AD patients; these alterations may be involved in compensatory mechanisms that could result from abnormalities in protein degradation, transport or distribution, which result from spine loss, among other factors (Leuba *et al.* 2008a,b). Furthermore, the function and localization of PSD95 are regulated through CDK5-mediated phosphorylation on its N-terminal (Morabito *et al.* 2004). This phosphorylation inhibits PSD95 multimerization and PSD95-mediated GluN channel recruitment. Interestingly, CDK5 inhibition prevented the aberrant PSD95 clusters, which was mimicked by p35 over-expression. However, CDK5 shRNA-miR-induced increases in PSD95 protein levels were identified *in vivo* in the context of neuroprotection, which suggests that increased postsynaptic contacts contributed to the reverse learning and memory impairment in AD mice. CDK5 regulates PSD95 ubiquitination through interactions with AP-, which suggests a mechanism in which PSD95 regulates GluN receptor-induced α-amino-3-hydroxy-5-methylisoxazole-4-propionate receptor endocytosis (Hawasli *et al.* 2007; Bianchetta *et al.* 2011). Together, these findings suggest that CDK5 and p35 have a fine regulation regarding the PSD95 levels and clustering, which may avoid excitotoxicity and promote plasticity.

3x-TgAD mice have demonstrated the loss of dendritic spines, in addition to intracellular βA and hyperphosphorylated tau (Bittner *et al.* 2010). Our previous studies indicate that CDK5 silencing directly affects the phosphorylation rate of tau (Piedrahita *et al.* 2010), reduces insoluble tau in the short and long term (Castro-Alvarez *et al.* 2014a), and involves the inhibition of GSK3β (Glycogen synthase kinase 3 beta) and phosphatases (Castro-Alvarez *et al.* 2014a,b, 2015). In addition, decreased toxicity via the reduction of active CDK5, the recovery of homeostasis, and the prevention of neuronal loss have been reported (Piedrahita *et al.* 2010), which may favor neuronal plasticity and the involvement of other factors. However, our current data provide new evidence that in a glutamate excitotoxicity context, there is an increase in calpain activity and AT8 when the p25 protein levels are increased and the p35 mRNA and protein levels are reduced, and these effects are prevented by CDK5 shRNA-miR. Interestingly, the silencing of p35 blocked CDK5 shRNA-miR-dependent protection, restoring the excitotoxicity of calpain activation without an increase in p25 and AT8 levels, as well as a reduction in the level of active Rac1 and a significant increase in RhoA activity, which suggest that p35 plays important role in neuronal survival and plasticity through Rho GTPase regulation.

In the previous decade, the investigation of the neuronal role of CDK5 in learning was limited by technical difficulties regarding the perinatal lethality of the constitutive knockout mice. However, the conditional knockout of the CDK5 in the adult mouse brain has enabled the demonstration that CDK5 suppression of approximately 50% in these mice improves performance in spatial learning tasks and enhances hippocampal long-term potentiation through GluN-mediated excitatory postsynaptic currents (Hawasli *et al.* 2007; Plattner *et al.* 2014). These previous results support our findings in which CDK5 silencing improves learning and memory in 3xTg-AD adult mice in the same brains with increased p35 and active Rac1, which maybe suggest a correlation of p35/Rac1 in survival and the consequent improvement of cognitive function. Additionally, to validate our observations, CDK5 pharmacological inhibition and the use of plasmids that over-express p35 have confirmed the specific effects of the used CDK5 shRNA-miR on p35 protein levels

and its effects on survival and plasticity, which supports p35 as CDK5 targets in mature neurons and the adult mouse brain.

In conclusion, p35 and Rho GTPases are molecular targets in the neuroprotection pathway induced by CDK5 RNAi. Upstream of Rho GTPases, p35 mainly function through Rac1 and RhoA, introducing a novel mechanism for the regulation of CDK5-induced neuroprotection that correlates with cognitive function recovery.

Acknowledgments and conflict of interest disclosure

The authors thank American Journal Experts for editing the English language in this manuscript, to thank Felipe Serrano for the graphical design, to Tania Marquez for assistance with the rat and mouse colonies at the SPF vivarium, Diego Alvarez for support regarding the mRNA analysis at the University of Antioquia, and Dr. Gary Bokoch (The Scripps Research Institute, La Jolla, CA, USA) and Dr. Jose Javier Lucas (Universidad Autonoma de Madrid, Spain) for the Rac1 and tTA construct donations, respectively. The research reported in this publication was supported by Colciencias, projects # 111545921503 and #111554531400, Mobility's project Colombia-Chile 576-2011 and PROLAB collaboration in Latin America/IBRO. In addition, this research was supported by the Fogarty International Center and the NIA NIH Institute under Award Number RO1-AG029802-01. The authors would like to thank the Advanced Microscopy Unit and the Viral Vector and Gene Therapy Unit from the Neuroscience Group of Antioquia, University of Antioquia. The content is solely the responsibility of the authors and does not necessarily represent the official views of the National Institutes of Health.

All experiments were conducted in compliance with the ARRIVE guidelines. The authors have no conflict of interest to declare.

Supporting information

Additional supporting information may be found in the online version of this article at the publisher's web-site:

Figure S1. Silencing of CDK5 reduces neurite branching in early neuronal primary cultures.

Figure S2. CDK5 inhibition protects against glutamate excitotoxicity: p35-dependent.

References

Bianchetta M. J., Lam T. T., Jones S. N. and Morabito M. A. (2011) Cyclin-dependent kinase 5 regulates PSD-95 ubiquitination in neurons. *J. Neurosci.* **31**, 12029–12035.

Bittner T., Fuhrmann M., Burgold S., Ochs S. M., Hoffmann N., Mitteregger G., Kretzschmar H., LaFerla F. M. and Herms J. (2010) Multiple events lead to dendritic spine loss in triple transgenic Alzheimer's disease mice. *PLoS ONE* **5**, e15477.

Bogush A., Pedrini S., Pelta-Heller J., Chan T., Yang Q., Mao Z., Sluzas E., Gieringer T. and Ehrlich M. E. (2007) AKT and CDK5/p35 mediate brain-derived neurotrophic factor induction of DARPP-32 in medium size spiny neurons in vitro. *J. Biol. Chem.* **282**, 7352–7359.

Castro-Alvarez J. F., Gutierrez-Vargas J., Darnaudery M. and Cardona-Gomez G. P. (2011) ROCK inhibition prevents tau hyperphosphorylation and p25/CDK5 increase after global cerebral ischemia. *Behav. Neurosci.* **125**, 465–472.

Castro-Alvarez J. F., Uribe-Arias S. A., Kosik K. S. and Cardona-Gomez G. P. (2014a) Long- and short-term CDK5 knockdown prevents spatial memory dysfunction and tau pathology of triple transgenic Alzheimer's mice. *Front. Aging Neurosci.* **6**, 243.

Castro-Alvarez J. F., Uribe-Arias S. A., Mejia-Raigosa D. and Cardona-Gomez G. P. (2014b) Cyclin-dependent kinase 5, a node protein in diminished tauopathy: a systems biology approach. *Front. Aging Neurosci.* **6**, 232.

Castro-Alvarez J. F., Uribe-Arias S. A. and Cardona-Gomez G. P. (2015) CDK5 targeting prevents ß-amyloid aggregation involving GSK3 ß and phosphatases. *J. Neurosci. Res.* In press.

Céspedes-Rubio A., Jurado F. W. and Cardona-Gómez G. P. (2010) p120 catenin/αN-catenin are molecular targets in the neuroprotection and neuronal plasticity mediated by atorvastatin after focal cerebral ischemia. *J. Neurosci. Res.* **88**, 3621–3634.

Cheung Z. H., Fu A. K. and Ip N. Y. (2006) Synaptic roles of Cdk5: implications in higher cognitive functions and neurodegenerative diseases. *Neuron* **50**, 13–18.

Cheung Z. H., Chin W. H., Chen Y., Ng Y. P. and Ip N. Y. (2007) Cdk5 is involved in BDNF-stimulated dendritic growth in hippocampal neurons. *PLoS Biol.* **5**, e63.

Cruz J. C., Tseng H. C., Goldman J. A., Shih H. and Tsai L. H. (2003) Aberrant Cdk5 activation by p25 triggers pathological events leading to neurodegeneration and neurofibrillary tangles. *Neuron* **40**, 471–483.

Darios F., Muriel M.-P., Khondiker M. E., Brice A. and Ruberg M. (2005) Neurotoxic calcium transfer from endoplasmic reticulum to mitochondria is regulated by cyclin-dependent kinase 5-dependent phosphorylation of tau. *J. Neurosci.* **25**, 4159–4168.

Dhavan R. and Tsai L.-H. (2001) A decade of CDK5. *Nat. Rev. Mol. Cell Biol.* **2**, 749–759.

Fu A. K. Y., Fu W.-Y., Cheung J., Tsim K. W. K., Ip F. C. F., Wang J. H. and Ip N. Y. (2001) Cdk5 is involved in neuregulin-induced AChR expression at the neuromuscular junction. *Nat. Neurosci.* **4**, 374–381.

Govek E. E., Newey S. E. and Van Aelst L. (2005) The role of the Rho GTPases in neuronal development. *Genes Dev.* **19**, 1–49.

Gutiérrez-Vargas J. A., Castro-Álvarez J. F., Velásquez-Carvajal D., Montañez-Velásquez M. N., Céspedes-Rubio A. and Cardona-Gómez G. P. (2010) Rac1 activity changes are associated with neuronal pathology and spatial memory long-term recovery after global cerebral ischemia. *Neurochem. Int.* **57**, 762–773.

Hall A. (1998) Rho GTPases and the actin cytoskeleton. *Science* **279**, 509–514.

Han P., Dou F., Li F., Zhang X., Zhang Y. W., Zheng H., Lipton S. A., Xu H. and Liao F. F. (2005) Suppression of cyclin-dependent kinase 5 activation by amyloid precursor protein: a novel excitoprotective mechanism involving modulation of tau phosphorylation. *J. Neurosci.* **25**, 11542–11552.

Harada T., Morooka T., Ogawa S. and Nishida E. (2001) ERK induces p35, a neuron-specific activator of Cdk5, through induction of Egr1. *Nat. Cell Biol.* **3**, 453–459.

Harris L. L., Talian J. C. and Zelenka P. S. (1992) Contrasting patterns of c-myc and N-myc expression in proliferating, quiescent, and differentiating cells of the embryonic chicken lens. *Development* **115**, 813–820.

Hawasli A. H., Benavides D. R., Nguyen C. *et al.* (2007) Cyclin-dependent kinase 5 governs learning and synaptic plasticity via control of NMDAR degradation. *Nat. Neurosci.* **10**, 880–886.

Hou Z., Li Q., He L., Lim H. Y., Fu X., Cheung N. S., Qi D. X. and Qi R. Z. (2007) Microtubule association of the neuronal p35 activator of Cdk5. *J. Biol. Chem.* **282**, 18666–18670.

Ittner L. M., Ke Y. D., Delerue F. *et al.* (2010) Dendritic function of tau mediates amyloid-beta toxicity in Alzheimer's disease mouse models. *Cell* **142**, 387–397.

Jaffe A. B. and Hall A. (2005) Rho GTPases: biochemistry and biology. *Annu. Rev. Cell Dev. Biol.* **21**, 247–269.

Jordan B. A., Fernholz B. D., Boussac M., Xu C., Grigorean G., Ziff E. B. and Neubert T. A. (2004) Identification and verification of novel rodent postsynaptic density proteins. *Mol. Cell Proteomics* **3**, 857–871.

Kerokoski P., Suuronen T., Salminen A., Soininen H. and Pirttilä T. (2004) Both N-methyl-d-aspartate (NMDA) and non-NMDA receptors mediate glutamate-induced cleavage of the cyclin-dependent kinase 5 (cdk5) activator p35 in cultured rat hippocampal neurons. *Neurosci. Lett.* **368**, 181–185.

Kesavapany S., Amin N., Zheng Y.-L. *et al.* (2004) p35/cyclin-dependent kinase 5 phosphorylation of ras guanine nucleotide releasing factor 2 (RasGRF2) mediates rac-dependent extracellular signal-regulated kinase 1/2 activity, altering RasGRF2 and microtubule-associated protein 1b distribution in neurons. *J. Neurosci.* **24**, 4421–4431.

Kusakawa G., Saito T., Onuki R., Ishiguro K., Kishimoto T. and Hisanaga S. (2000) Calpain-dependent proteolytic cleavage of the p35 cyclin-dependent kinase 5 activator to p25. *J. Biol. Chem.* **275**, 17166–17172.

Lee J.-H. and Kim K.-T. (2004) Induction of cyclin-dependent kinase 5 and its activator p35 through the extracellular-signal-regulated kinase and protein kinase A pathways during retinoic-acid mediated neuronal differentiation in human neuroblastoma SK-N-BE(2)C cells. *J. Neurochem.* **91**, 634–647.

Leuba G., Savioz A., Vernay A., Carnal B., Kraftsik R., Tardif E., Riederer I. and Riederer B. M. (2008a) Differential changes in synaptic proteins in the Alzheimer frontal cortex with marked increase in PSD-95 postsynaptic protein. *J. Alzheimers Dis.* **15**, 139–151.

Leuba G., Walzer C., Vernay A., Carnal B., Kraftsik R., Piotton F., Marin P., Bouras C. and Savioz A. (2008b) Postsynaptic density protein PSD-95 expression in Alzheimer's disease and okadaic acid induced neuritic retraction. *Neurobiol. Dis.* **30**, 408–419.

Leuba G., Vernay A., Kraftsik R., Tardif E., Riederer B. M. and Savioz A. (2014) Pathological reorganization of NMDA receptors subunits and postsynaptic protein PSD-95 distribution in Alzheimer's disease. *Curr. Alzheimer Res.* **11**, 86–96.

Lew J., Huang Q. Q., Qi Z., Winkfein R. J., Aebersold R., Hunt T. and Wang J. H. (1994) A brain-specific activator of cyclin-dependent kinase 5. *Nature* **371**, 423–426.

Li B. S., Sun M. K., Zhang L., Takahashi S., Ma W., Vinade L., Kulkarni A. B., Brady R. O. and Pant H. C. (2001) Regulation of NMDA receptors by cyclin-dependent kinase-5. *Proc. Natl Acad. Sci. USA* **98**, 12742–12747.

Li B.-S., Ma W., Jaffe H., Zheng Y., Takahashi S., Zhang L., Kulkarni A. B. and Pant H. C. (2003) Cyclin-dependent kinase-5 Is involved in neuregulin-dependent activation of phosphatidylinositol 3-kinase and Akt activity mediating neuronal survival. *J. Biol. Chem.* **278**, 35702–35709.

Linseman D. A. and Loucks F. A. (2008) Diverse roles of Rho family GTPases in neuronal development, survival, and death. *Front Biosci.* **13**, 657–676.

Liu F., Su Y., Li B., Zhou Y., Ryder J., Gonzalez-DeWhitt P., May P. C. and Ni B. (2003) Regulation of amyloid precursor protein (APP) phosphorylation and processing by p35/Cdk5 and p25/Cdk5. *FEBS Lett.* **547**, 193–196.

Lopes J. P., Oliveira C. R. and Agostinho P. (2007) Role of cyclin-dependent kinase 5 in the neurodegenerative process triggered by amyloid-Beta and prion peptides: implications for Alzheimer's disease and prion-related encephalopathies. *Cell. Mol. Neurobiol.* **27**, 943–957.

Ma T., Zhao Y., Kwak Y.-D., Yang Z., Thompson R., Luo Z., Xu H. and Liao F.-F. (2009) Statin's excitoprotection is mediated by sAPP and the subsequent attenuation of calpain-induced truncation events, likely via rho-ROCK signaling. *J. Neurosci.* **29**, 11226–11236.

Mann D. M., Iwatsubo T., Cairns N. J. *et al.* (1996) Amyloid beta protein (Abeta) deposition in chromosome 14-linked Alzheimer's disease: predominance of Abeta 42(43). *Ann. Neurol.* **40**, 149–156.

Morabito M. A., Sheng M. and Tsai L. H. (2004) Cyclin-dependent kinase 5 phosphorylates the N-terminal domain of the postsynaptic density protein PSD-95 in neurons. *J. Neurosci.* **24**, 865–876.

Nguyen K. C., Rosales J. L., Barboza M. and Lee K. Y. (2002) Controversies over p25 in Alzheimer's disease. *J. Alzheimers Dis.* **4**, 123–126.

Nikolic M., Chou M. M., Lu W., Mayer B. J. and Tsai L.-H. (1998) The p35/Cdk5 kinase is a neuron-specific Rac effector that inhibits Pak1 activity. *Nature* **395**, 194–198.

Noble W., Olm V., Takata K. *et al.* (2003) Cdk5 is a key factor in tau aggregation and tangle formation in vivo. *Neuron* **38**, 555–565.

Oddo S., Caccamo A., Shepherd J. D. *et al.* (2003) Triple-transgenic model of Alzheimer's Disease with plaques and tangles: intracellular Abeta and synaptic dysfunction. *Neuron* **39**, 409–421.

Ohshima T., Ogura H., Tomizawa K. *et al.* (2005) Impairment of hippocampal long-term depression and defective spatial learning and memory in p35 mice. *J. Neurochem.* **94**, 917–925.

Park K. H., Lu G., Fan J., Raymond L. A. and Leavitt B. R. (2012) Decreasing levels of the cdk5 activators, p25 and p35, reduces excitotoxicity in striatal neurons. *J. Huntingtons Dis.*, **1**.

Patrick G. N., Zhou P., Kwon Y. T., Howley P. M. and Tsai L.-H. (1998) p35, the Neuronal-specific Activator of Cyclin-dependent Kinase 5 (Cdk5) Is Degraded by the Ubiquitin-Proteasome Pathway. *J. Biol. Chem.* **273**, 24057–24064.

Patrick G. N., Zukerberg L., Nikolic M., de la Monte S., Dikkes P. and Tsai L. H. (1999) Conversion of p35 to p25 deregulates Cdk5 activity and promotes neurodegeneration. *Nature* **402**, 615–622.

Peng J., Kim M. J., Cheng D., Duong D. M., Gygi S. P. and Sheng M. (2004) Semiquantitative proteomic analysis of rat forebrain postsynaptic density fractions by mass spectrometry. *J. Biol. Chem.* **279**, 21003–21011.

Piedrahita D., Hernandez I., Lopez-Tobon A. *et al.* (2010) Silencing of CDK5 reduces neurofibrillary tangles in transgenic alzheimer's mice. *J. Neurosci.* **30**, 13966–13976.

Plattner F., Hernandez A., Kistler T. M. *et al.* (2014) Memory enhancement by targeting Cdk5 regulation of NR2B. *Neuron* **81**, 1070–1083.

Posada-Duque R. A., Velasquez-Carvajal D., Eckert G. P. and Cardona-Gomez G. P. (2013) Atorvastatin requires geranylgeranyl transferase-I and Rac1 activation to exert neuronal protection and induce plasticity. *Neurochem. Int.* **62**, 433–445.

Putkonen N., Kukkonen J. P., Mudo G., Putula J., Belluardo N., Lindholm D. and Korhonen L. (2011) Involvement of cyclin-dependent kinase-5 in the kainic acid-mediated degeneration of glutamatergic synapses in the rat hippocampus. *Eur. J. Neurosci.* **34**, 1212–1221.

Querfurth H. W. and LaFerla F. M. (2010) Alzheimer's disease. *N. Engl. J. Med.* **362**, 329–344.

Read D. E. and Gorman A. M. (2009) Involvement of Akt in neurite outgrowth. *Cell. Mol. Life Sci.* **66**, 2975–2984.

Saito T., Konno T., Hosokawa T., Asada A., Ishiguro K. and Hisanaga S. (2007) p25/cyclin-dependent kinase 5 promotes the progression of cell death in nucleus of endoplasmic reticulum-stressed neurons. *J. Neurochem.* **102**, 133–140.

Sananbenesi F., Fischer A., Wang X., Schrick C., Neve R., Radulovic J. and Tsai L. H. (2007) A hippocampal Cdk5 pathway regulates extinction of contextual fear. *Nat. Neurosci.* **10**, 1012–1019.

Semenova M. M., Maki-Hokkonen A. M., Cao J., Komarovski V., Forsberg K. M., Koistinaho M., Coffey E. T. and Courtney M. J. (2007) Rho mediates calcium-dependent activation of p38alpha and subsequent excitotoxic cell death. *Nat. Neurosci.* **10**, 436–443.

Shirao T. and Gonzalez-Billault C. (2013) Actin filaments and microtubules in dendritic spines. *J. Neurochem.* **126**, 155–164.

Shukla V., Zheng Y. L., Mishra S. K., Amin N. D., Steiner J., Grant P., Kesavapany S. and Pant H. C. (2013) A truncated peptide from p35, a Cdk5 activator, prevents Alzheimer's disease phenotypes in model mice. *FASEB J.* **27**, 174–186.

Smith D. S., Greer P. L. and Tsai L. H. (2001) Cdk5 on the brain. *Cell Growth Differ.* **12**, 277–283.

Su S. C. and Tsai L. H. (2011) Cyclin-dependent kinases in brain development and disease. *Annu. Rev. Cell Dev. Biol.* **27**, 465–491.

Tada T. and Sheng M. (2006) Molecular mechanisms of dendritic spine morphogenesis. *Curr. Opin. Neurobiol.* **16**, 95–101.

Takahashi S., Ohshima T., Cho A. *et al.* (2005) Increased activity of cyclin-dependent kinase 5 leads to attenuation of cocaine-mediated dopamine signaling. *Proc. Natl Acad. Sci. USA* **102**, 1737–1742.

Tanaka T., Veeranna, Ohshima T. *et al.* (2001) Neuronal cyclin-dependent kinase 5 activity is critical for survival. *J. Neurosci.*, **21**, 550–558.

Timsit S. and Menn B. (2012) Cyclin-dependent kinase inhibition with roscovitine: neuroprotection in acute ischemic stroke. *Clin. Pharmacol. Ther.* **91**, 327–332.

Tokuoka H., Saito T., Yorifuji H., Wei F., Kishimoto T. and Hisanaga S. (2000) Brain-derived neurotrophic factor-induced phosphorylation of neurofilament-H subunit in primary cultures of embryo rat cortical neurons. *J. Cell Sci.* **113**(Pt 6), 1059–1068.

Trapp T., Olah L., Holker I., Besselmann M., Tiesler C., Maeda K. and Hossmann K. A. (2001) GTPase RhoB: an early predictor of neuronal death after transient focal ischemia in mice. *Mol. Cell Neurosci.* **17**, 883–894.

Trunova S. and Giniger E. (2012) Absence of the Cdk5 activator p35 causes adult-onset neurodegeneration in the central brain of Drosophila. *Dis. Model. Mech.* **5**, 210–219.

Tsai L.-H., Delalle I., Caviness V. S., Chae T. and Harlow E. (1994) p35 is a neural-specific regulatory subunit of cyclin-dependent kinase 5. *Nature* **371**, 419–423.

Tsujita Y., Muraski J., Shiraishi I., Kato T., Kajstura J., Anversa P. and Sussman M. A. (2006) Nuclear targeting of Akt antagonizes aspects of cardiomyocyte hypertrophy. *Proc. Natl Acad. Sci. USA* **103**, 11946–11951.

Tymianski M. (2011) Emerging mechanisms of disrupted cellular signaling in brain ischemia. *Nat. Neurosci.* **14**, 1369–1373.

Utreras E., Henriquez D., Contreras-Vallejos E., Olmos C., Di Genova A., Maass A., Kulkarni A. B. and Gonzalez-Billault C. (2013) Cdk5 regulates Rap1 activity. *Neurochem. Int.* **62**, 848–853.

Wang J., Liu S., Fu Y., Wang J. H. and Lu Y. (2003) Cdk5 activation induces hippocampal CA1 cell death by directly phosphorylating NMDA receptors. *Nat. Neurosci.* **6**, 1039–1047.

Wang C. X., Song J. H., Song D. K., Yong V. W., Shuaib A. and Hao C. (2005) Cyclin-dependent kinase-5 prevents neuronal apoptosis through ERK-mediated upregulation of Bcl-2. *Cell Death Differ.* **13**, 1203–1212.

Wei F. Y., Tomizawa K., Ohshima T. *et al.* (2005) Control of cyclin-dependent kinase 5 (Cdk5) activity by glutamatergic regulation of p35 stability. *J. Neurochem.* **93**, 502–512.

Zhang L., Liu W., Szumlinski K. K. and Lew J. (2012) p10, the N-terminal domain of p35, protects against CDK5/p25-induced neurotoxicity. *Proc. Natl Acad. Sci. USA* **109**, 20041–20046.

Zhang X., Hermandez I., Rei D. *et al.* (2013) Diaminothiazoles modify tau phosphorylation and improve the tauopathy in mouse models. *J. Biol. Chem.*, **30**, 22042–22056.

Zheng Y. L., Kesavapany S., Gravell M., Hamilton R. S., Schubert M., Amin N., Albers W., Grant P. and Pant H. C. (2005) A Cdk5 inhibitory peptide reduces tau hyperphosphorylation and apoptosis in neurons. *EMBO J.* **24**, 209–220.

Zheng Y. L., Li B. S., Kanungo J., Kesavapany S., Amin N., Grant P. and Pant H. C. (2007) Cdk5 Modulation of mitogen-activated protein kinase signaling regulates neuronal survival. *Mol. Biol. Cell* **18**, 404–413.

Zheng Y. L., Amin N. D., Hu Y. F. *et al.* (2010) A 24-residue peptide (p5), derived from p35, the Cdk5 neuronal activator, specifically inhibits Cdk5-p25 hyperactivity and tau hyperphosphorylation. *J. Biol. Chem.* **285**, 34202–34212.

Zhou Y., Su Y., Li B. *et al.* (2003) Nonsteroidal anti-inflammatory drugs can lower amyloidogenic Abeta42 by inhibiting Rho. *Science* **302**, 1215–1217.

Zhu H., Bhattacharyya B. J., Lin H. and Gomez C. M. (2011) Skeletal muscle IP3R1 receptors amplify physiological and pathological synaptic calcium signals. *J. Neurosci.* **31**, 15269–15283.